

TUNABLE COLOR CORRECTION BETWEEN LINEAR AND POLYNOMIAL MODELS FOR NOISY IMAGES

Ryo Yamakabe, Yusuke Monno, Masayuki Tanaka, and Masatoshi Okutomi

Tokyo Institute of Technology

ABSTRACT

Linear color correction (LCC) and polynomial color correction (PCC) are widely used in a camera imaging pipeline. PCC generally achieves lower colorimetric errors than LCC. However, if an image contains noise, PCC amplifies the noise more severely than LCC. Consequently, there is a trade-off between LCC and PCC in the presence of noise. In this paper, we propose a novel framework for color correction, which we call tunable color correction (TCC). TCC enables us to tune a color correction matrix between linear and polynomial models by a tuning parameter. We also present a way of selecting a suitable parameter value based on the mean squared error calculation model for PCC. Experimental results demonstrate that TCC effectively balances the trade-off and outperforms both LCC and PCC for noisy images.

Index Terms— Color correction, linear model, polynomial model, noise

1. INTRODUCTION

In color digital cameras, the spectral sensitivity functions of RGB color filters are device-dependent and usually differ from those of the human visual system. Thus, color correction (or camera characterization) is an essential process that transforms a camera-dependent RGB color space into a standard or desired color space, typically the device-independent XYZ or display sRGB color space [1, 2].

Many color correction methods were proposed in the past literatures, including least-squares regression-based methods [2–5], look-up-table-based methods [6, 7], and neural network-based methods [8, 9]. Among these methods, linear color correction (LCC) [2, 3] and polynomial color correction (PCC) [4] are widely used. LCC is performed by multiplying a camera RGB vector by a 3×3 LCC matrix. PCC exploits high-order terms in addition to the first-order linear terms used in LCC. Both in LCC and PCC, the color correction matrix is calculated by least-squares regression (often with some constraint [10–13]) to minimize the colorimetric errors between target and color-corrected values for training data.

One challenge of LCC and PCC is to reduce the amplification of image noise while keeping high color fidelity. PCC generally achieves lower colorimetric errors than LCC, thanks to the use of the high-order terms. However, PCC amplifies

noise more severely than LCC, because the high-order terms in PCC generally have large noise variance. Consequently, there is a trade-off between LCC and PCC regarding color fidelity and noise amplification.

Effects of noise on color measurement systems are analyzed in the literatures of spectral sensitivity designs [14–16] and color correction [17–21]. These works are based on the mean squared error (MSE) calculation model for LCC. The literatures [17–21] provide ways of calculating an optimal LCC matrix regarding the MSE in the presence of noise. However, to the best of our knowledge, none of existing works explicitly derive the MSE calculation model for PCC.

In this paper, we propose a novel framework for color correction, which we call tunable color correction (TCC). TCC enables us to tune a color correction matrix between linear and polynomial models by a tuning parameter, and thus enables us to balance the trade-off between LCC and PCC. We also present a way of selecting a suitable parameter value based on the MSE calculation model for PCC, which we explicitly derive for the first time. Experimental results demonstrate that TCC outperforms LCC and PCC for noisy images.

2. GENERAL FORMULATION OF LCC AND PCC

LCC and PCC are generally formulated in a matrix form as

$$\mathbf{q} = \mathbf{M}\mathbf{p}, \quad (1)$$

where $\mathbf{p} \in \mathbb{R}^N$ is an input vector formed by camera RGB values, $\mathbf{q} \in \mathbb{R}^3$ is an output color-corrected vector in a target color space, and $\mathbf{M} \in \mathbb{R}^{3 \times N}$ is a color correction matrix. The dimension of \mathbf{p} depends on how many terms are used for the color correction. Hereafter, we consider that LCC and PCC include the bias term. The input vector of LCC is formed as

$$\mathbf{p}_{lcc} = [1, p_R, p_G, p_B]^T, \quad (2)$$

where p_R , p_G , and p_B are camera intensity values of R, G, and B channels, respectively. PCC uses high-order terms. In what follows, we focus on the second-order PCC with the bias term to design our proposed TCC. The input vector of the second-order PCC is formed as

$$\mathbf{p}_{pcc2} = [1, p_R, p_G, p_B, p_R p_G, p_G p_B, p_B p_R, p_R^2, p_G^2, p_B^2]^T. \quad (3)$$

The color correction matrix is typically calculated using training color patches by least-squares regression as

$$\hat{\mathbf{M}} = \arg \min_{\mathbf{M}} \|\mathbf{Q}_t - \mathbf{M}\mathbf{P}_t\|_F^2, \quad (4)$$

where $\|\cdot\|_F$ is the Frobenius norm, $\mathbf{Q}_t \in \mathbb{R}^{3 \times K}$ is a matrix containing the color vectors of K training patches in the target color space, $\mathbf{P}_t \in \mathbb{R}^{N \times K}$ is a matrix containing the corresponding input vectors formed by the camera RGB values of the patches. The matrix $\hat{\mathbf{M}} \in \mathbb{R}^{3 \times N}$ is calculated to minimize the average colorimetric error for the training patches, typically by using noise-free camera RGB values of the patches obtained in a color calibration phase. However, that matrix amplifies noise when applied to noisy images [17–22].

3. PROPOSED TUNABLE COLOR CORRECTION

3.1. Color correction matrix calculation

Our proposed TCC is motivated by the fact that large color correction coefficients for high-order terms in PCC result in large noise amplification, as will be shown in subsection 3.3. This fact leads us to calculate our proposed TCC matrix as

$$\hat{\mathbf{M}}(\lambda) = \arg \min_{\mathbf{M}} \left(\|\mathbf{Q}_t - \mathbf{M}\mathbf{P}_t\|_F^2 + \frac{1}{\lambda} \|\mathbf{W} \circ \mathbf{M}\|_F^2 \right), \quad (5)$$

where $\hat{\mathbf{M}}(\lambda) \in \mathbb{R}^{3 \times N}$ is the TCC matrix, which is the same size as the PCC matrix. The first term is the data fidelity term, which is the same as Eq. (4). The second term is our proposed constrain term, where \circ represents the element-wise product and $\mathbf{W} \in \mathbb{R}^{3 \times N}$ is a binary weighting matrix designed to constrain on the coefficients for the high-order terms. Specifically, in the case of the second-order form of Eq. (3), the weighting matrix is designed as

$$\mathbf{W} = \begin{bmatrix} 0 & 0 & 0 & 0 & 1 & 1 & 1 & 1 & 1 & 1 \\ 0 & 0 & 0 & 0 & 1 & 1 & 1 & 1 & 1 & 1 \\ 0 & 0 & 0 & 0 & 1 & 1 & 1 & 1 & 1 & 1 \end{bmatrix}. \quad (6)$$

Our proposed TCC matrix has the following properties.

$$\begin{aligned} \lim_{\lambda \rightarrow 0} \hat{\mathbf{M}}(\lambda) &= [\hat{\mathbf{M}}_{lcc} \mid \mathbf{0}], \\ \lim_{\lambda \rightarrow \infty} \hat{\mathbf{M}}(\lambda) &= \hat{\mathbf{M}}_{pcc}, \end{aligned} \quad (7)$$

where $\hat{\mathbf{M}}_{lcc} \in \mathbb{R}^{3 \times 4}$ and $\hat{\mathbf{M}}_{pcc} \in \mathbb{R}^{3 \times N}$ are the LCC and PCC matrices calculated by Eq. (4), respectively. $\mathbf{0}$ is the zero matrix of size $3 \times (N - 4)$. Those properties indicate that TCC is tunable between LCC and PCC by a parameter λ .

Eq. (5) can be solved in the vectorized form as

$$\hat{\mathbf{m}}_v(\lambda) = \left(\mathbf{P}_v^T \mathbf{P}_v + \frac{1}{\lambda} \mathbf{W}_d^T \mathbf{W}_d \right)^{-1} \mathbf{P}_v^T \mathbf{q}_v, \quad (8)$$

where $\hat{\mathbf{m}}_v(\lambda) \in \mathbb{R}^{3N}$ and $\mathbf{q}_v \in \mathbb{R}^{3K}$ are the vectorized form of $\hat{\mathbf{M}}(\lambda)$ and \mathbf{Q}_t , respectively. $\mathbf{P}_v \in \mathbb{R}^{3K \times 3N}$ is the matrix representing the input vectors. $\mathbf{W}_d \in \mathbb{R}^{3N \times 3N}$ is the diagonal matrix whose diagonal elements are the weights in \mathbf{W} .

3.2. Selection of the parameter value

In this subsection, we present a way of selecting the parameter value based on the MSEs for training color patches. In the presence of noise, the MSE for the k -th patch is estimated as

$$MSE_k(\lambda) = E(\|\mathbf{q}_k - \hat{\mathbf{M}}(\lambda)\mathbf{p}_k\|_2^2), \quad (9)$$

where $E(\cdot)$ is the expectation operator, \mathbf{q}_k is the target vector for the k -th patch, and \mathbf{p}_k is a random variable representing the input vector with noise. Let $\boldsymbol{\mu}_k \in \mathbb{R}^N$ be the expectation of \mathbf{p}_k , i.e., $\boldsymbol{\mu}_k = E(\mathbf{p}_k)$. Then, Eq. (9) can be rewritten as

$$MSE_k(\lambda) = \|\mathbf{q}_k - \hat{\mathbf{M}}(\lambda)\boldsymbol{\mu}_k\|_2^2 + \sum_{i=1}^3 V(\hat{\mathbf{m}}_i^T(\lambda)\mathbf{p}_k), \quad (10)$$

where $\hat{\mathbf{m}}_i(\lambda) \in \mathbb{R}^N$ is the vector representing the i -th row of $\hat{\mathbf{M}}(\lambda)$, i.e., $\hat{\mathbf{M}}(\lambda) = [\hat{\mathbf{m}}_1(\lambda), \hat{\mathbf{m}}_2(\lambda), \hat{\mathbf{m}}_3(\lambda)]^T$, and $V(\cdot)$ is the variance operator. The first term represents the expected colorimetric error. The second term represents the noise variance of the color-corrected values. The expected vector $\boldsymbol{\mu}_k$ and the noise variance to calculate the MSE will be modeled in the next subsection.

Based on the MSE for each training color patch, the value of the tuning parameter λ is selected as

$$\hat{\lambda} = \arg \min_{\lambda} \sum_{k=1}^K MSE_k(\lambda), \quad (11)$$

where $\hat{\lambda}$ minimizes the sum of the MSEs for all patches.

3.3. MSE calculation model

Equation (10) indicates that the MSE for each training patch can be calculated from the expected vector $\boldsymbol{\mu}_k$ and the noise variance of the color-corrected values. Such calculations are widely performed in LCC [17–21]. However, to the best of our knowledge, none of existing works have extended the calculations to PCC. In what follows, we derive the MSE calculation model for the second-order PCC, which is used to design our proposed TCC in Eq. (5). Hereafter, we denote the second-order PCC as PCC for notation simplicity.

We first derive the expectation of the input vector, \mathbf{p}_{pcc_2} in Eq. (3). If an input image contains noise, the camera RGB values can be represented as

$$p_R = g_R + n_R, \quad p_G = g_G + n_G, \quad p_B = g_B + n_B, \quad (12)$$

where g_R , g_G , and g_B are latent noise-free camera RGB values, and n_R , n_G , and n_B represent noise of each channel, respectively.

In the following discussion, we assume that noise of each channel is zero-mean signal-independent Gaussian noise and the noise variance of each channel is σ_R^2 , σ_G^2 , or σ_B^2 . We further assume that the noise of each channel is independent

of the latent noise-free RGB values and independent of each other. These assumptions are often made in the past literatures [14, 20]. Based on those assumptions, the expectation of the input vector, $\boldsymbol{\mu}_{pcc_2} = E(\mathbf{p}_{pcc_2})$, is derived as

$$\boldsymbol{\mu}_{pcc_2} = [1, g_R, g_G, g_B, g_R g_G, g_G g_B, g_B g_R, g_R^2 + \sigma_R^2, g_G^2 + \sigma_G^2, g_B^2 + \sigma_B^2]^T. \quad (13)$$

We next derive the noise variance of color-corrected values by PCC. To simplify the notation, we rewrite Eq. (3) as

$$\mathbf{p}_{pcc_2} = [1, p_R, p_G, p_B, p_R p_G, p_G p_B, p_B p_R, p_R^2, p_G^2, p_B^2]^T \\ = [1, p_R, p_G, p_B, p_{RG}, p_{GB}, p_{BR}, p_{R^2}, p_{G^2}, p_{B^2}]^T.$$

Then, we express the color-corrected vector by PCC as

$$\mathbf{q} = [q_1, q_2, q_3]^T = \mathbf{M}_{pcc_2} \mathbf{p}_{pcc_2}, \\ = [\mathbf{m}_1^T \mathbf{p}_{pcc_2}, \mathbf{m}_2^T \mathbf{p}_{pcc_2}, \mathbf{m}_3^T \mathbf{p}_{pcc_2}]^T, \quad (14)$$

where \mathbf{m}_i is the vector representing the i -th row of the PCC matrix, i.e., $\mathbf{M}_{pcc_2} = [\mathbf{m}_1, \mathbf{m}_2, \mathbf{m}_3]^T$.

Hereafter, without loss of generality, we omit the row index i for notation simplicity and express the vector \mathbf{m}_i as

$$\mathbf{m} = [m_1, m_R, m_G, m_B, m_{RG}, m_{GB}, m_{BR}, m_{R^2}, m_{G^2}, m_{B^2}]^T.$$

Then, a color-corrected value by PCC is expressed as

$$q = \mathbf{m}^T \mathbf{p}_{pcc_2} \\ = m_1 + m_R p_R + m_G p_G + m_B p_B \\ + m_{RG} p_{RG} + m_{GB} p_{GB} + m_{BR} p_{BR} \\ + m_{R^2} p_{R^2} + m_{G^2} p_{G^2} + m_{B^2} p_{B^2}. \quad (15)$$

In the following formulation, we let $X \in \{R, G, B\}$ be the index set of the first-order linear terms, $XY \in \{RG, GB, BR\}$ be that of the second-order cross terms, and $X^2 \in \{R^2, G^2, B^2\}$ be that of the squared terms. Similarly, we use (X, Y) , (XY, YZ) , (X^2, Y^2) , (X, XY) , (X, X^2) , and (XY, X^2) to represent sets of all possible combinations of the linear, cross, and squared terms. Then, the noise variance of the color-corrected value by PCC is derived as

$$V(q) = \sum_X m_X^2 V(p_X) + \sum_{XY} m_{XY}^2 V(p_{XY}) + \sum_{X^2} m_{X^2}^2 V(p_{X^2}) \\ + 2 \left(\sum_{(X,Y)} m_X m_Y C(p_X, p_Y) + \sum_{(XY,YZ)} m_{XY} m_{YZ} C(p_{XY}, p_{YZ}) \right. \\ + \sum_{(X^2,Y^2)} m_{X^2} m_{Y^2} C(p_{X^2}, p_{Y^2}) + \sum_{(X,XY)} m_X m_{XY} C(p_X, p_{XY}) \\ \left. + \sum_{(X,X^2)} m_X m_{X^2} C(p_X, p_{X^2}) + \sum_{(XY,X^2)} m_{XY} m_{X^2} C(p_{XY}, p_{X^2}) \right). \quad (16)$$

where $C(\cdot, \cdot)$ is the covariance operator. By using the assumptions we made, the variance and the covariance in

Eq. (16) are derived as $V(p_X) = \sigma_X^2$, $V(p_{XY}) = g_X^2 \sigma_Y^2 + g_Y^2 \sigma_X^2 + \sigma_X^2 \sigma_Y^2$, $V(p_{X^2}) = 2\sigma_X^4 + 4g_X^2 \sigma_X^2$, $C(p_X, p_Y) = 0$, $C(p_{XY}, p_{YZ}) = g_X g_Z \sigma_Y^2$, $C(p_{X^2}, p_{Y^2}) = 0$, $C(p_X, p_{XY}) = g_Y \sigma_X^2$, $C(p_X, p_{X^2}) = 2g_X \sigma_X^2$, and $C(p_{XY}, p_{X^2}) = 2g_X g_Y \sigma_X^2$, respectively.

In the above calculations, we derived the variance and the covariance of the second-order-related terms, which are generally large values. These calculation results motivate us to design the weighting matrix for TCC as Eq. (6) to constrain on the coefficients for the second-order terms.

Finally, the MSE for each training patch can be calculated by Eq. (10) using the derived models in Eq. (13) and (16).

3.4. Procedure of our proposed TCC

The procedure of our proposed TCC is summarized as follows. In the matrix calculation phase, training color patches are captured as bright as possible to get the noise-free camera RGB values (i.e., g_R , g_G , and g_B) of the patches. Then, TCC matrices are calculated by Eq. (5) using a set of parameter values ($\lambda = \lambda_1, \lambda_2, \dots$). In the application phase, the MSE for each training patch is calculated using Eq. (10), (13), and (16) for given noise levels (i.e., σ_R , σ_G , and σ_B), which are assumed to be known or estimated from the captured image [23]. Then, the best parameter value $\hat{\lambda}$ is selected by Eq. (11). Finally, the TCC matrix with the selected parameter value is applied to the captured noisy image.

4. EXPERIMENTAL RESULTS

We conducted simulation experiments to evaluate the performance of LCC, PCC, and our proposed TCC. For the calculation of the color correction matrices, we used the spectral reflectance data of 96 patches in the X-lite ColorChecker Digital SG as training data. We set the target color space to the sRGB color space and used the CIE A illumination as a light source for generating camera RGB values.

From the spectral reflectance data of the 96 patches, the target color vectors in the sRGB color space (to construct \mathbf{Q}_t) were generated using XYZ color matching functions and the XYZ-to-sRGB transformation matrix. Noise-free camera RGB values under the CIE A illumination (to construct \mathbf{P}_t) were generated using the Olympus E-PL2 camera sensitivity [24]. The LCC and PCC matrices were calculated by Eq. (4). Our proposed TCC matrices were calculated by Eq. (5) using a set of tuning parameter values. In the following experiments, we assumed that the noise variance is the same for all channels, i.e., $\sigma_R^2 = \sigma_G^2 = \sigma_B^2 = \sigma^2$.

We first show the effects of different parameter values on TCC. Figure 1 shows the results of the MSE calculation by Eq. (10) for the TCC matrices with different parameter values. Each result in Fig. 1 shows the average of all 96 training patches with $\sigma = 4$. Figure 1 (a) shows the calculated colorimetric error, which corresponds to the root of the first term of Eq. (10). Figure 1 (b) shows the calculated standard

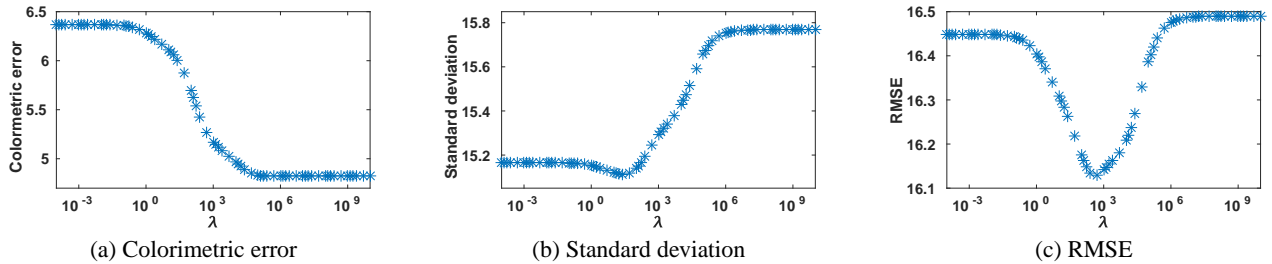


Fig. 1. Results of the MSE calculation by Eq. (10) for our proposed TCC matrices with different parameter values. Each result shows the average of all 96 training patches with $\sigma = 4$. (a) Colorimetric error, (b) standard deviation of noise, and (c) RMSE. Note that LCC and PCC are equivalent to the cases of $\lim \lambda \rightarrow 0$ and $\lim \lambda \rightarrow \infty$, respectively.

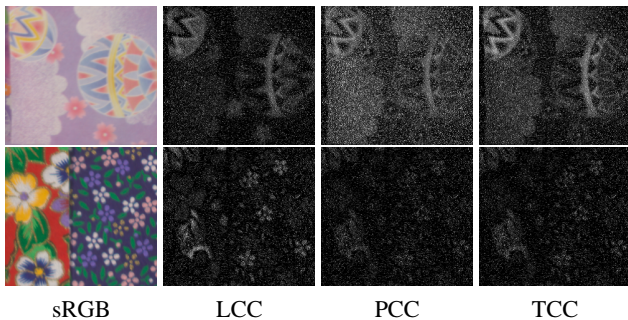


Fig. 2. Comparison of the RMSE maps ($\sigma = 2$). The contrast is enhanced for visualization. The result of PCC in the top row shows the large noise variance, while the result of LCC in the bottom row shows the large colorimetric errors. Our TCC provides the balanced results between LCC and PCC.

deviation of noise, which corresponds to the root of the second term of Eq. (10). Figure 1 (c) shows the calculated root MSE (RMSE), which corresponds to the root of Eq. (10).

In Fig. 1, LCC and PCC are equivalent to the cases of $\lim \lambda \rightarrow 0$ and $\lim \lambda \rightarrow \infty$, respectively. Fig. 1 (a) shows that the colorimetric error of PCC ($\lim \lambda \rightarrow \infty$) is lower than that of LCC ($\lim \lambda \rightarrow 0$). This is because of the advantage of using the high-order terms in PCC. In contrast, Fig. 1 (b) shows that the standard deviation of the color-corrected values by PCC is larger than that by LCC. This is because the high-order terms in PCC cause large noise amplification.

Fig. 1 (a) and (b) show that our proposed TCC transitionally moves between LCC and PCC by changing the parameter value. Fig. 1 (c) further indicates that there is a point that balances the trade-off between LCC and PCC, and yields the result with the minimum RMSE. In TCC, the parameter value corresponding to that point can be selected based on the MSE calculation model for the training patches, which we derived in Eq. (10), (13), and (16).

We next evaluate the performance of TCC. For this purpose, we used two test datasets: synthesized 96 ColorChecker SG patches (200×200 samples for each patch) and 30 hyperspectral images in [25]. The first dataset were used to simulate an ideal case that the training and test data are the same. The

Table 1. Average RMSE comparison.

σ	ColorChecker SG			Hyperspectral		
	LCC	PCC	TCC	LCC	PCC	TCC
0	6.37	4.81	4.81	11.30	10.65	10.65
2	9.91	9.24	9.17	13.61	13.24	13.29
4	16.45	16.49	16.13	18.91	19.00	18.83
6	23.62	24.17	23.41	25.40	25.92	25.32
8	31.00	31.99	30.81	32.37	33.30	32.25
10	38.43	39.88	38.23	39.57	40.94	39.44

second dataset were used to simulate a more realistic case that the training and test data are different.

The average RMSEs for both datasets are shown in Table 1. For the noise-free and low-noise cases ($\sigma = 0, 2$), TCC provides the results similar to those of PCC, which are better than LCC. With the increase of the noise level, the average RMSEs of PCC becomes larger than those of LCC due to the noise amplification. In contrast, TCC generally provides better results than both LCC and PCC for various noise levels.

Figure 2 shows the visual comparison of the RMSE maps for the hyperspectral dataset. The result of PCC in the top row shows the large noise variance, while the result of LCC in the bottom row shows the large colorimetric errors. In contrast, TCC provides the balanced results between LCC and PCC. Both the numerical and visual comparisons validate that our proposed TCC can effectively balance the trade-off regarding color fidelity and noise amplification.

5. CONCLUSION

In this paper, we proposed TCC, which enables us to tune a color correction matrix between linear and polynomial models by a tuning parameter, and thus enables us to balance the trade-off between LCC and PCC. We also presented a way of selecting a suitable parameter value based on the MSE model for PCC. Experimental results demonstrated that our proposed TCC outperforms LCC and PCC for noisy images.

Acknowledgment. This work was partly supported by the MIC/SCOPE #141203024.

6. REFERENCES

- [1] M. Anderson, R. Motta, S. Chandrasekar, and M. Stokes, "Proposal for a standard default color space for the internet - sRGB," *Proc. of Color and Imaging Conference (CIC)*, pp. 238–245, 1996.
- [2] H. R. Kang, *Computational color technology*, SPIE Press, 2006.
- [3] P. M. Hubel, J. Holm, G. D. Finlayson, and M. S. Drew, "Matrix calculations for digital photography," *Proc. of Color and Imaging Conference (CIC)*, pp. 105–111, 1997.
- [4] G. Hong, M. R. Luo, and P. A. Rhodes, "A study of digital camera colorimetric characterisation based on polynomial modelling," *Color Research and Application*, vol. 26, no. 1, pp. 76–84, 2001.
- [5] G. D. Finlayson, M. Mackiewicz, and A. Hurlbert, "Colour correction using root-polynomial regression," *IEEE Trans. on Image Processing*, vol. 24, no. 5, pp. 1460–1470, 2015.
- [6] P. C. Hung, "Colorimetric calibration in electronic imaging devices using a look-up-table model and interpolations," *Journal of Electronic Imaging*, vol. 2, no. 1, pp. 53–61, 1993.
- [7] J. S. McElvain and W. Gish, "Camera color correction using two-dimensional transforms," *Proc. of Color and Imaging Conference (CIC)*, pp. 250–256, 2013.
- [8] H. R. Kang and P. G. Anderson, "Neural network applications to the color scanner and printer calibrations," *Journal of Electronic Imaging*, vol. 1, no. 2, pp. 125–135, 1992.
- [9] V. Cheung, S. Westland, D. Connah, and C. Ripamonti, "A comparative study of the characterisation of colour cameras by means of neural networks and polynomial transforms," *Coloration Technology*, vol. 120, no. 1, pp. 19–25, 2004.
- [10] G. D. Finlayson and M. S. Drew, "Constrained least-squares regression in color spaces," *Journal of Electronic Imaging*, vol. 6, no. 4, pp. 484–493, 1997.
- [11] H. Zhang and H. Liu, "Hue constrained matrix optimization for preferred color reproduction," *Journal of Electronic Imaging*, vol. 21, no. 3, pp. 033021–1–15, 2012.
- [12] C. F. Andersen and D. Connah, "Weighted constrained hue-plane preserving camera characterization," *IEEE Trans. on Image Processing*, vol. 25, no. 9, pp. 4329–4339, 2016.
- [13] M. Mackiewicz, C. F. Andersen, and G. D. Finlayson, "Method for hue plane preserving color correction," *J. Opt. Soc. Am. A*, vol. 33, no. 11, pp. 2166–2177, 2016.
- [14] M. J. Vrhel and H. J. Trussell, "Optimal color filters in the presence of noise," *IEEE Trans. on Image Processing*, vol. 4, no. 6, pp. 814–823, 1995.
- [15] P. Vora and C. Herley, "Trade-offs between color saturation and noise sensitivity in image sensors," *Proc. of IEEE Int. Conf. on Image Processing (ICIP)*, pp. 196–200, 1998.
- [16] N. Shimano, "Suppression of noise effects in color correction by spectral sensitivities of image sensors," *Optical Review*, vol. 9, no. 2, pp. 81–88, 2002.
- [17] Y. P. Tan and T. Acharya, "A method for color correction with noise consideration," *Proc. of SPIE*, vol. 3963, pp. 329–337, 2000.
- [18] U. Barnhöfer, J. DiCarlo, B. Olding, and B. Wandell, "Color estimation error trade-offs," *Proc. of SPIE*, vol. 5017, pp. 263–273, 2003.
- [19] S. Quan, "Analytical approach to the optimal linear matrix with comprehensive error metric," *Proc. of SPIE*, vol. 5292, pp. 243–253, 2004.
- [20] S. Lim and A. Silverstein, "Spatially varying color correction (SVCC) matrices for reduced noise," *Proc. of Color and Imaging Conference (CIC)*, pp. 76–81, 2004.
- [21] H. J. Trussell and M. J. Vrhel, "Color estimation under Poisson noise," *Proc. of IEEE Int. Conf. on Acoustics, Speech and Signal Processing (ICASSP)*, pp. 1914–1918, 2013.
- [22] K. Takahashi, Y. Monno, M. Tanaka, and M. Okutomi, "Effective color correction pipeline for a noisy image," *Proc. of IEEE Int. Conf. on Image Processing (ICIP)*, pp. 4002–4006, 2016.
- [23] X. Liu, M. Tanaka, and M. Okutomi, "Single-image noise level estimation for blind denoising," *IEEE Trans. on Image Processing*, vol. 22, no. 12, pp. 5226–5237, 2013.
- [24] J. Jiang, D. Liu, J. Gu, and S. Süsstrunk, "What is the space of spectral sensitivity functions for digital color cameras?," *Proc. of Workshop on Applications of Computer Vision (WACV)*, pp. 168–179, 2013.
- [25] Y. Monno, S. Kikuchi, M. Tanaka, and M. Okutomi, "A practical one-shot multispectral imaging system using a single image sensor," *IEEE Trans. on Image Processing*, vol. 24, no. 10, pp. 3048–3059, 2015.